

## Scaffolds of PDLA/Bioglass 58S Produced via Selective Laser Sintering

Rafaela do Vale Pereira<sup>a\*</sup>, Gean Vitor Salmoria<sup>b</sup>,

Marcela Oliveira Caldeira de Moura<sup>a</sup>, Águedo Aragones<sup>c</sup>, Márcio Celso Fredel<sup>a</sup>

<sup>a</sup>CERMAT, Mechanical Engineering Department,  
Federal University of Santa Catarina – UFSC, Florianópolis, SC, Brazil

<sup>b</sup>CIMJECT, Mechanical Engineering Department,  
Federal University of Santa Catarina – UFSC, Florianópolis, SC, Brazil

<sup>c</sup>Odontology Department, Federal University of Santa Catarina – UFSC, Florianópolis, SC, Brazil

Received: June 20, 2013; Revised: May 5, 2014

Scaffolds of PDLA were produced to be implemented in maxillofacial surgeries inducing bone repair and regeneration. To prepare these scaffolds, bioglass (BG58S) was synthesized by sol-gel method, in order to be applied as osteoconductive dispersed particles in PDLA matrix. Once presenting greater facility on parts fabrication, this polymeric matrix enables complex geometries production besides presenting compatible degradation rate for scaffold absorption and bone regeneration. Scaffolds production was performed by selective laser sintering in order to obtain tailored-made parts. FTIR and XRD analyses were carried out to observe the composition and evaluate the presence of crystalized phases in bioglass, obtaining Wollastonite. SEM was used to observe the BG particle distribution in PDLA matrix and flexural test was performed to evaluate the composite mechanical properties. Results showed that was possible to obtain pieces using SLS method and with addition of 10%wt BG to polymeric matrix, flexural modulus and strength increased regarding to pure polymer.

**Keywords:** scaffold, bioglass, PDLA, selective laser sintering (SLS).

### 1. Introduction

In Tissue engineering, materials science is combined with medicine and biology in order to make improvements in the human beings life by providing techniques to reconstruct damaged tissues and organs<sup>1</sup>. A common technique used for these purpose is scaffold implantation at the injured parts, using adequate materials that promote tissue regeneration.

Biodegradable polymers are widely used, nevertheless, their degradation residues decrease the medium pH, turning it acid, promoting an undesirable inflammatory response. In order to minimize this inflammatory response, bioactive ceramic particles are incorporated to the matrix, stabilizing the medium pH. BG 58S (60%SiO<sub>2</sub>, 36%CaO, 4%P<sub>2</sub>O<sub>5</sub> (% mol)), a resorbable biomaterial, was used as dispersed particles in polymer matrix in order to promote osteoconduction and pH stabilization, aiding bone regeneration. These regeneration is due to calcium and phosphate ions release, which are present at BG composition and play an important role at bone metabolism (angiogenesis, grow and tissue mineralization)<sup>2-6</sup>.

Scaffolds can be prepared by Selective Laser Sintering (SLS), a Rapid Prototyping (RP) manufacturing technology, which is able to produce tailored-made parts for each fracture. This method is based at material powder sinterization, layer-by-layer, by an infrared laser beam (CO<sub>2</sub> Laser), which produces a final part previously obtained by computer-aided design (CAD). Other advantages of

this technique are high dimensional accuracy, allowing well defined details, and achievement of complex designs. Once scaffolds require controlled properties and structure (as interconnected porosity and 3D structure, to allow cell migration, nutrition and proliferation), SLS is a widely used fabrication method<sup>7,8</sup>.

In order to optimize samples processing with SLS method, (optimizing microstructure, mechanical properties and surface characteristics of the scaffolds), some variables can be controlled: laser power, scan speed and spot diameter at focus. These variables estimate the laser energy density (Equation 1) that reaches the material surface<sup>9-14</sup>.

$$\rho_e = P / (v \cdot d) \quad (1)$$

where  $\rho_e$  (J/mm<sup>2</sup>) is the laser energy density, P (W) is the laser power, v (mm/s) is the scan speed and d (mm) is the spot diameter.

This study presents scaffolds production to be used at non-load bearing areas, as, for example, facial skeleton<sup>15</sup>. To produce these scaffolds two biomaterial were combined, poly (D,L) lactide (PDLA) and bioglass 58S (BG 58S). PDLA was the composite matrix, hence is a biomaterial that can be applied in non-load bearing due to its mechanical characteristics and complete resorption after within 72 weeks of implantation<sup>15</sup>.

Four compositions of sample (0%wt BG, 10%wt BG, 20%wt BG and 30%wt BG) were prepared and the aim

\*e-mail: rafaelavpereira@gmail.com

of this study was to produce samples by SLS method, confirm if the synthesized materials presented the correct composition and structure and investigate the influence of BG particles amount at the mechanical properties of these composites.

2. Material and Methods

PDLLA was synthesized (as described in<sup>16</sup>) and provided by Biomaterials Laboratory from Medical and Biological Science Center of Pontifical Catholic University (PUC-Sorocaba, SP).

BG 58S was synthesized by the author via sol-gel process. For that, were used Tetraethyl orthosilicate (TEOS) (Sigma Aldrich, reagente grade 98%, 131903-11, lot STBB8489V), to obtain silica. Triethyl phosphate (TEP) (Sigma Aldrich, 99.8%, 538728-11, lot MKBC5090). Calcium nitrate tetrahydrate ( $\text{Ca}(\text{NO}_3)_2 \cdot 4 \text{H}_2\text{O}$ ) (Vetec, cod. 000663.08, lot 1006753). Nitric acid ( $\text{HNO}_3$ ) (Vetec, 68%, cod. 000451.06, lot 0903829), to control solution pH and ethyl alcohol (Synth, P.A.-A.C.S., lot A1084.01.BJ), used as solution solvent.

2.1. Synthesis of sol-gel process

BG58S was synthesized by sol-gel process as follows. At first TEOS, TEP and  $(\text{Ca}(\text{NO}_3)_2 \cdot 4 \text{H}_2\text{O})$  (with BG58S molar ratio), ethanol and 2M  $\text{HNO}_3$  were added in an Erlenmeyer, at 50 °C and constant agitation. Solution was placed in a stove (Drying and sterilizing stove, Nova Ética, 402/D) at 70 °C for 24h in order to dry the material and promote its gelation.

Subsequently the material was thermally treated at 600 °C and milled in an eccentric mill (BP Engenharia, CB2-T), producing a material with  $d_{50} = 12.15 \mu\text{m}$  (Mastersizer 2000, Malvern Instruments), used as dispersed particles at the polymeric matrix of composite. Also, with this powder, FTIR (Spectrophotometer Bruker, Tensor 27) and XRD (Vertical diffractometer, Philips, PW1150) were performed.

2.2. Sample preparation at SLS

In order to prepare samples for mechanical analyses, PDLLA in pellets was milled in an industrial blender (Stainless steel Industrial Blender, TRON, 25000 rpm), with liquid nitrogen, achieving a range of particles between 150  $\mu\text{m}$  and 300  $\mu\text{m}$  (sieve analysis), which is indicated to obtain the necessary scaffolds porosity<sup>17,18</sup>.

PDLLA and BG powder were mixed at a Y-mixer for 45 min, in different proportions, 10%wt BG, 20%wt BG and 30%wt BG. The different compositions were processed at

SLS (Table 1) producing samples with rectangular shape (35.0 × 5.0 × 2.3 mm).

Laser power of 5.4W was used at the process, once lower power didn't promote the particles sinterization and higher powder promoted polymer degradation.

These rectangular samples were tested at DMA (Q800, TA Instruments) with single cantilever at 30 °C with an increase stress rate of 2N/min, obtaining stress-strain curves.

2.3. Characterizations

In order to characterize the materials, some tests were realized. For BG 58S FTIR (Bruker Spectrophotometer, Tensor 27) was carried out with sample prepared as a pastille of BG and KBR. Also XRD (Vertical diffractometer, Philips, PW1150) in which BG powder was analyzed.

For PDLLA were carried out: Gel permeation chromatography (GPC) (Schmadzu, UFLC), polymer powder was solubilized at THF; FTIR (Bruker Spectrophotometer, Tensor 27), sample was prepared as a PDLLA pastille; Nuclear magnetic Resonance (NMR) (Varian, NMR AS 400) and Differential Scanning Calorimetry (DSC) (Shimadzu, DSC – 50) with initial temperature of 20 °C heating rate of 5 °C/min until 200 °C ( $\text{N}_2$  purge).

3. Results and Discussion

3.1. BG Characterization

The observed infrared spectrum obtained for BG58S is presented at Figure 1. The peak at  $465\text{cm}^{-1}$  refers to Si-O-Si bending mode, at  $601\text{cm}^{-1}$  refers to P-O bending vibration of  $\text{PO}_4^{3-}$  tetrahedral in crystalline HCA (carbonated hydroxyapatite), probably resulting of a reaction from BG powder and atmospheric moisture. The slope about  $930\text{cm}^{-1}$  is associated to the Si-O-Ca vibration mode. Region around  $1045\text{cm}^{-1}$  refers to both Si-O-Si asymmetric stretching mode and P-O stretching vibration. 1395 and  $1647\text{cm}^{-1}$  present carbonates bands and  $3410\text{cm}^{-1}$  (not shown in graphic) refers to hydroxyl band<sup>2,19-21</sup>.

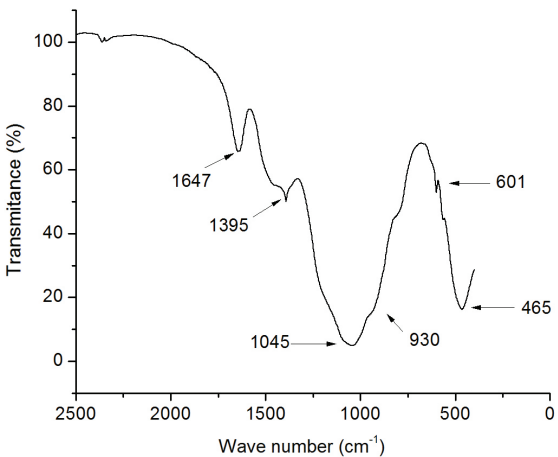


Figure 1. BG58S FTIR spectrum.

Table 1. Compositions and laser power for sample processing.

Composition	Power (W)	Sample name
Pure polymer	5.4	00BG5,4
10%wt of BG	5.4	10BG5,4
20%wt of BG	5.4	20BG5,4
30%wt of BG	5.4	30BG5,4

Figure 2 presents BG58S XRD spectrum, showing the amorphous region and a peak at  $2\theta$  equal to 34, indicating the presence of wollastonite ( $\text{CaSiO}_3$ ) crystalline phase. Wollastonite presents great influence at biomaterials activity, aiding at the formation of carbonated apatite layer, which provides the bonding with osseous tissue<sup>19,22</sup>.

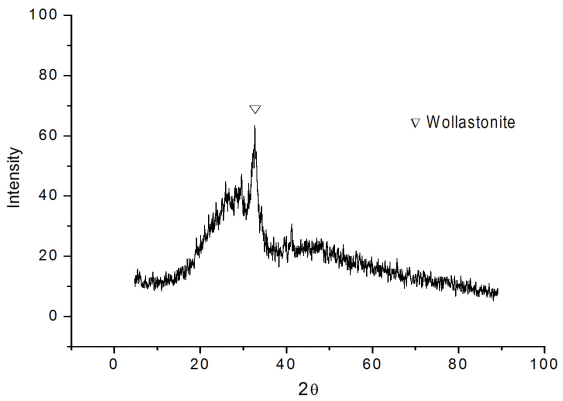


Figure 2. BG58S XRD spectrum.

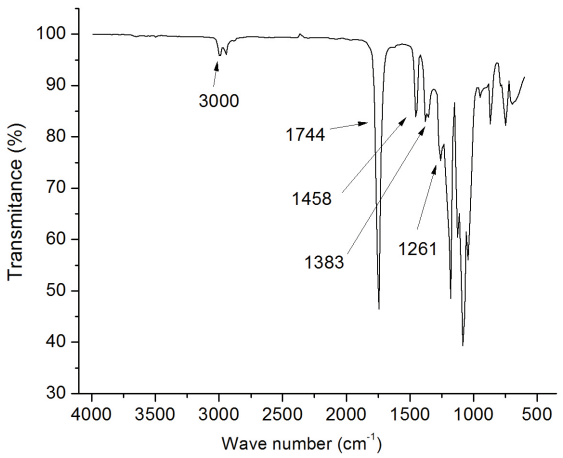


Figure 3. PDLLA FTIR spectrum.

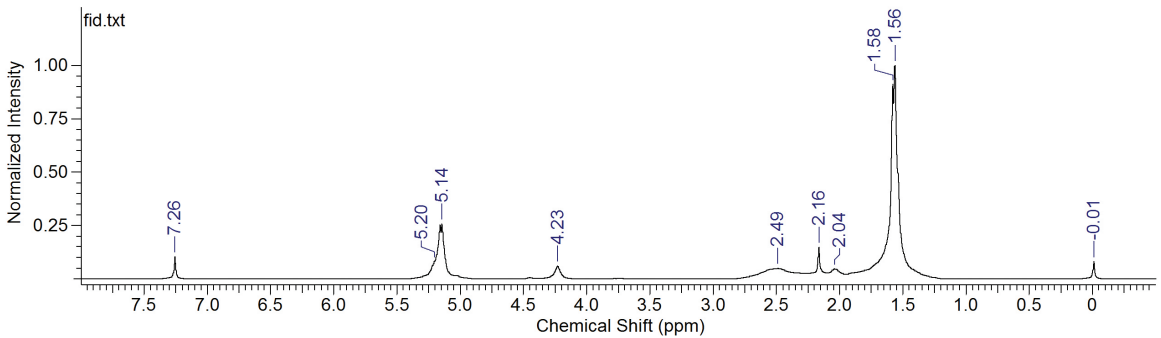


Figure 4.  $^1\text{H}$ -NMR PDLLA spectrum.

### 3.2. PDLLA characterization

The composite matrix was produced with the synthesized PDLLA and its composition and properties were analyzed by GPC, FTIR, DSC and NMR.

Molecular mass was measured by gel permeation chromatography (GPC) and the values for Mn (78498 g/mol), Mw (153596 g/mol) and polydispersity index (1.95) were obtained.

Figure 3 presents FTIR spectrum for PDLLA. First notable peaks are at  $3000$  and  $2943\text{ cm}^{-1}$ , which refer to C-H stretching bonds, due to methyl and methyne groups. At  $1744\text{ cm}^{-1}$ , are presented the stretching mode of the carboxyl groups.  $1458\text{ cm}^{-1}$  are presented the  $\text{CH}_3$  asymmetric deformation modes. Peak at  $1383\text{ cm}^{-1}$  represents the  $\delta_s\text{CH}_3$  symmetric deformation.  $1261\text{ cm}^{-1}$  refers to stretching modes of ester groups  $-\text{CO}-\text{O}-$ <sup>[16,23,24]</sup>. These presented peaks characterize important groups of PDLLA molecular structure, showing that the synthesized polymer's structure is in accordance to literature<sup>16,24</sup>.

Figure 4 presents  $^1\text{H}$  NMR spectrum of PDLLA using  $\text{CDCl}_3$ . The doublet peak at  $1.56\text{ ppm}$  represents the  $-\text{CH}_3$  protons; the multiple at  $5.14\text{ ppm}$  represent the  $-\text{CH}$  groups present in polymer chain and  $7.26\text{ ppm}$  the  $-\text{OH}$  groups<sup>16,23,24</sup>.

Figure 5 represents the  $^{13}\text{C}$ -NMR PDLLA spectrum using  $\text{CDCl}_3$ . Peak at  $16.61\text{ ppm}$  represents  $-\text{CH}_3$  groups; at  $68.98\text{ ppm}$  the  $-\text{CH}$  groups and at  $169.63\text{ ppm}$ ,  $-\text{COOH}$  groups<sup>16,24</sup>.

In both NMR spectra were identified the important groups of the molecular structure, showing that the synthesized PDLLA presents the correct structure as in literature<sup>16,24</sup>.

Figure 6 presents DSC graphic of amorphous PDLLA where is observed the polymer  $T_g$  at  $42^\circ\text{C}$ . The regular values for PDLLA are between  $50$  and  $60^\circ\text{C}$ <sup>[16,23]</sup>.

### 3.3. Composite characterization

In order to characterize the mechanical behavior of composites, DMA was used and the graphic of stress-strain was obtained. Three samples of each composition were tested and the average values of modulus were recorded at 1 till 3% strain. The results are presented at Figure 7. Table 2 presents the composition of each sample, as well as the average Flexural Modulus ( $E_{\text{average}}$ ), average Maximum Strength ( $\sigma_{\text{average}}$ ) and Rupture Strain ( $\epsilon_{\text{rupture}}$ ).

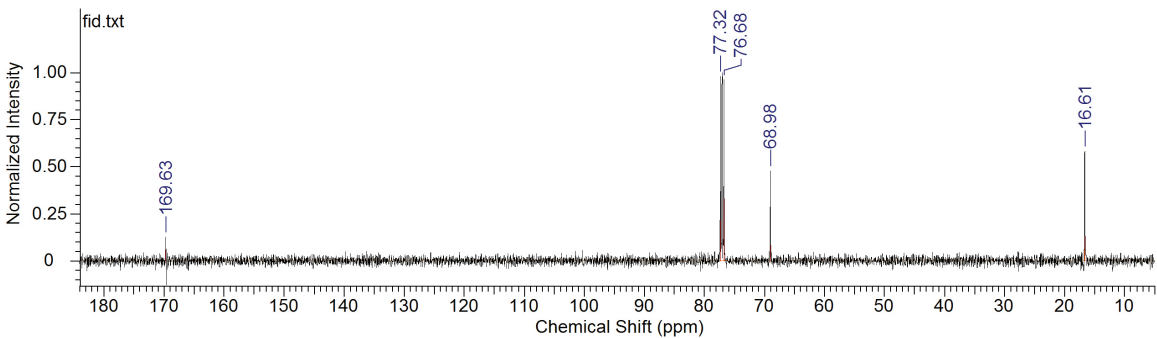


Figure 5. <sup>13</sup>C-NMR PDLLA spectrum.

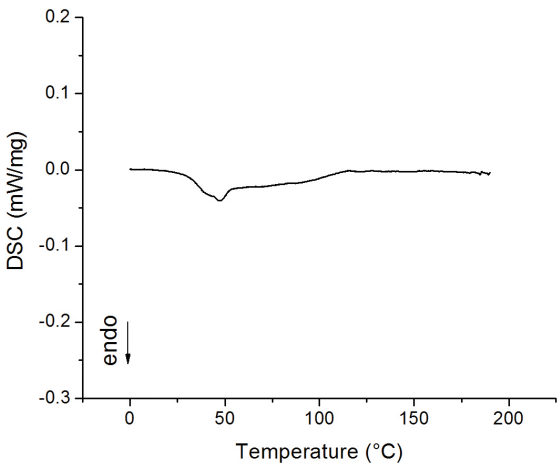


Figure 6. DSC graphic of PDLLA.

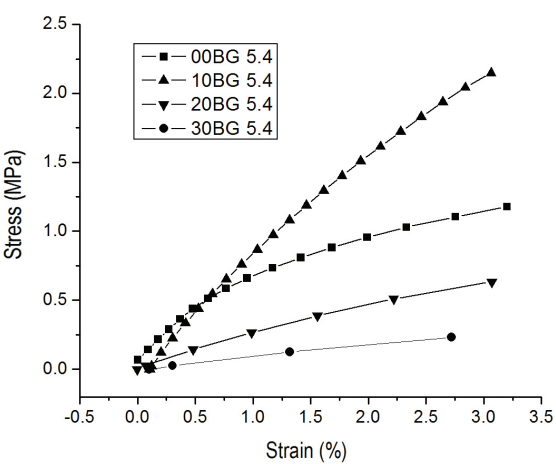


Figure 7. Stress-strain curve for PDLLA/BG58S composites.

Table 2. Name, composition and flexural properties values of the scaffolds.

Sample	%wt of BG	E <sub>average</sub> (MPa)	σ <sub>average</sub> (3%ε)	ε <sub>rupture</sub> (%)
00BG 5,4	00	68.07±16.16	1.04±0.05	>25
10BG 5,4	10	79.00±23.75	1.68±0.45	>06
20BG 5,4	20	20.88±11.87	0.61±0.03	>04
30BG 5,4	30	10.09±08.39	0.22±0.16	>03

For values until 3% of strain, composite with 10%wt of BG obtained the higher values of average flexural modulus and also higher values for average maximum strength. Nevertheless, the samples with pure polymer presented strain values for rupture considerably higher than composite with 10%wt of BG. The composites with higher amounts of BG (20 and 30%wt) presented a significant decrease of values for flexural modulus, maximum strength and rupture strain.

3.4. Scanning Electron Microscopy (SEM)

Each composition of samples was taken to SEM and micrographs of 50 and 200x of magnification were taken (Figures 8 and 9). (Research supported by LCME-UFSC.) As can be seen at composite micrographs, it is possible to observe that for pure polymer, necks were formed and particles sinterization occurred. The addition of bioglass particles (10, 20 and 30%wt of BG)

interfered at neck formation between the polymer particles, preventing polymer sinterization. These samples were also analyzed by computed tomography (Metrotom 1500, Zeiss, LABMETRO/UFSC), which confirmed the pores interconnectivity (data not shown).

4. Conclusions

Bioglass 58S analyses by FTIR and XDR stated the composition and structure compatible to the literature, showing that the BG synthesis by sol-gel process was accurate. FTIR and NMR of PDLLA attested the composition and structure of the synthesized polymer.

The composites were able to be produced via SLS method, presenting interconnected porous microstructure, specially, for pure polymer. Nevertheless less intense neck formation was observed with bioglass addition.

Stress-strain curves for PDLLA composites with 10%wt of BG presented greater values for flexural modulus and



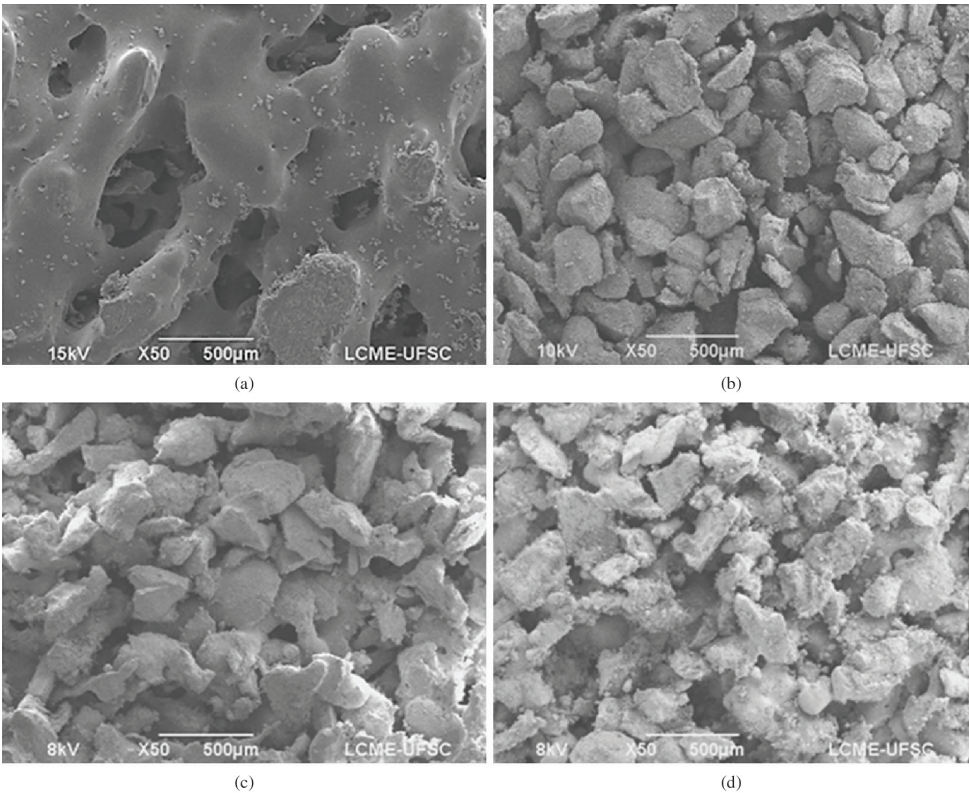


**Figure 8.** Micrographs with 50x of magnification. a) pure polymer; b) polymer with 10%wt of BG; c) polymer with 20%wt of BG; d) polymer with 30%wt of BG.

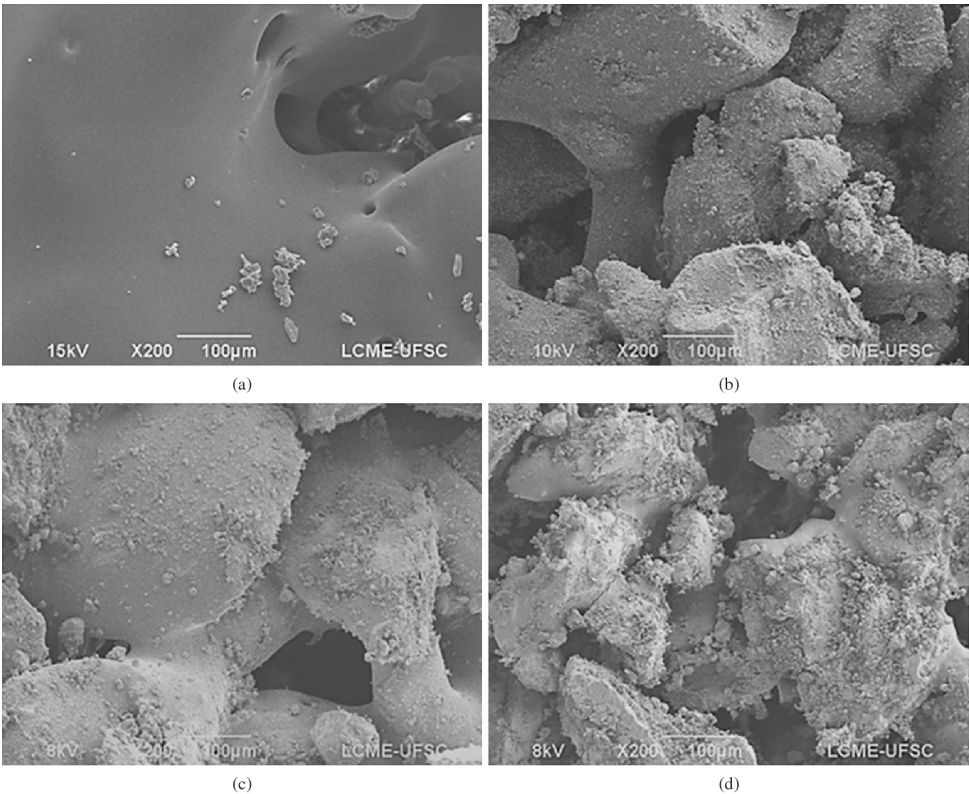


**Figure 9.** Micrographs with 200x of magnification. a) pure polymer; b) polymer with 10%wt of BG; c) polymer with 20%wt of BG; d) polymer with 30%wt of BG.

strength. However, for composites with higher BG amounts these values decreased due to a decrease in the polymer particles coalescence.

PDLLA/BG58S composites were able to be produced by SLS method, presenting the most relevant results for 10%wt of BG.

## References

- Barbanti SH, Zavaglia CAC and Duek EAR. Polímeros bioreabsorvíveis na engenharia de tecidos. *Polímeros*. 2005; 15:13-21. <http://dx.doi.org/10.1590/S0104-14282005000100006>
- Zhong J and Greenspan DC. Processing and properties of sol-gel bioactive glasses. *Journal of Biomedical Materials Research*. 2000; 53(6):694-701. [http://dx.doi.org/10.1002/1097-4636\(2000\)53:6<694::AID-JBM12>3.0.CO;2-6](http://dx.doi.org/10.1002/1097-4636(2000)53:6<694::AID-JBM12>3.0.CO;2-6)
- Santos DV, Casadei APM, Pereira RV, Aragones A, Salmoria GV and Fredel MF. Development of Polymer/nanoceramic Composite Material with Potential Application in Biomedical Engineering. *Materials Science Forum*. 2012; 727-728:1142-1146. <http://dx.doi.org/10.4028/www.scientific.net/MSF.727-728.1142>
- Blaker JJ, Nazhat SN, Maquet V and Boccaccini AR. Long-term in vitro degradation of PDLLA/bioglass bone scaffolds in acellular simulated body fluid. *Acta Biomaterialia*. 2011; 7(2):829-40. PMID:20849987. <http://dx.doi.org/10.1016/j.actbio.2010.09.013>
- Sepulveda P, Jones JR and Hench LL. Characterization of melt-derived 45S5 and sol-gel-derived 58S bioactive glasses. *Journal of Biomedical Materials Research*. 2001; 58(6):734-40. PMID:11745528. <http://dx.doi.org/10.1002/jbm.10026>
- Hoppe A, Guldal NS and Boccaccini AR. A review of the biological response to ionic dissolution products from bioactive glasses and glass-ceramics. *Biomaterials*. 2011; 32(11):2757-2774. PMID:21292319. <http://dx.doi.org/10.1016/j.biomaterials.2011.01.004>
- Salmoria GV, Ahrens CH, Klauss P, Paggi RA, Oliveira RG and Lago A. Rapid manufacturing of polyethylene parts with controlled pore size gradients using selective laser sintering. *Materials Research*. 2007; 10:211-214. <http://dx.doi.org/10.1590/S1516-14392007000200019>
- Loh QL and Choong C. Three-dimensional scaffolds for tissue engineering applications: Role of porosity and pore size. *Tissue Engineering - Part B: Reviews*. 2013; 19(6):485-502. PMID:23672709. <http://dx.doi.org/10.1089/ten.teb.2012.0437>
- Salmoria GV, Klauss P, Paggi RA, Kanis LA and Lago A. Structure and mechanical properties of cellulose based scaffolds fabricated by selective laser sintering. *Polymer Testing*. 2009; 28(6):648-652. <http://dx.doi.org/10.1016/j.polymertesting.2009.05.008>
- Salmoria GV, Paggi RA, Lago A and Beal VE. Microstructural and mechanical characterization of PA12/MWCNTs nanocomposite manufactured by selective laser sintering. *Polymer Testing*. 2011; 30(6):611-615. <http://dx.doi.org/10.1016/j.polymertesting.2011.04.007>
- Savalani MM, Hao L, Zhang Y, Tanner KE and Harris RA. Fabrication of porous bioactive structures using the selective laser sintering technique. *Proceedings of the Institution of Mechanical Engineers Part H-Journal of Engineering in Medicine*. 2007; 221(H8):873-886. PMID:18161247. <http://dx.doi.org/10.1243/09544119JEIM232>
- Kruth J-P, Mercelis P, Van Vaerenbergh J, Froyen L and Rombouts M. Binding Mechanisms in Selective Laser Sintering and Selective Laser Melting. *Rapid Prototyping Journal*. 2005; 26-36. <http://dx.doi.org/10.1108/13552540510573365>
- Antonov EN, Bagratashvili VN, Whitaker MJ, Barry JJ, Shakesheff KM, Kononov AN et al. Three-Dimensional Bioactive and Biodegradable Scaffolds Fabricated by Surface-Selective Laser Sintering. *Advanced Materials*. 2005; 17(3):327-330. PMID:17464361 PMID:PMC1855444. <http://dx.doi.org/10.1002/adma.200400838>
- Sharma VS, Singh S, Sachdeva A and Kumar P. Influence of sintering parameters on dynamic mechanical properties of selective laser sintered parts. *International Journal of Material Forming*. 2013; 1-10.
- Heidemann W, Jeschkeit-Schubbert S, Ruffieux K, Fischer JH, Jung H, Krueger G et al. pH-stabilization of predegraded PDLLA by an admixture of water-soluble sodiumhydrogenphosphate—results of an in vitro- and in vivo-study. *Biomaterials*. 2002; 23(17):3567-3574. [http://dx.doi.org/10.1016/S0142-9612\(02\)00046-7](http://dx.doi.org/10.1016/S0142-9612(02)00046-7)
- Motta AC and Duek EAR. Síntese e caracterização do copolímero poli (L-co-D,L Ácido Láctico). *Polímeros*. 2007; 17:123-129. <http://dx.doi.org/10.1590/S0104-14282007000200011>
- Karageorgiou V and Kaplan D. Porosity of 3D biomaterial scaffolds and osteogenesis. *Biomaterials*. 2005; 26(27):5474-91. PMID:15860204. <http://dx.doi.org/10.1016/j.biomaterials.2005.02.002>
- Chen Q, Roether JA and Boccaccini AR. Tissue Engineering Scaffolds from Bioactive Glass and Composite Materials. In: Ashammakhi N, Reis R and Chiellini F, editors. Topics in tissue engineering, vol. 4. 2008.
- Balamurugan A, Sockalingum G, Michel J, Fauré J, Banchet V, Wortham L et al. Synthesis and characterisation of sol gel derived bioactive glass for biomedical applications. *Materials Letters*. 2006; 60(29-30):3752-3757. <http://dx.doi.org/10.1016/j.matlet.2006.03.102>
- Sepulveda P, Jones JR and Hench LL. In vitro dissolution of melt-derived 45S5 and sol-gel derived 58S bioactive glasses. *Journal of Biomedical Materials Research*. 2002; 61(2):301-11. PMID:12007211. <http://dx.doi.org/10.1002/jbm.10207>
- Arcos D, Greenspan DC and Vallet-Regi M. Influence of the stabilization temperature on textural and structural features and ion release in SiO<sub>2</sub>-CaO-P<sub>2</sub>O<sub>5</sub> sol-gel glasses. *Chemistry of Materials*. 2002; 14(4):1515-1522. <http://dx.doi.org/10.1021/cm011119p>
- Jones JR, Ehrenfried LM and Hench LL. Optimising bioactive glass scaffolds for bone tissue engineering. *Biomaterials*. 2006; 27(7):964-73. PMID:16102812. <http://dx.doi.org/10.1016/j.biomaterials.2005.07.017>
- Kaitian X, Kozluca A, Denkbaz EB and Piskin E. Poly (D,L-lactic acid) homopolymers: Synthesis and characterization. *Turkish Journal of Chemistry*. 1996; 20(1):43-53.
- Proiakakis CS, Mamouzelos NJ, Tarantili PA and Andreopoulos AG. Stability of DL-poly(lactic acid) in aqueous solutions. *Journal of Applied Polymer Science*. 2003; 87(5):795-804. <http://dx.doi.org/10.1002/app.11449>